Continental Shelf Research 177 (2019) 24–32

Contents lists available at ScienceDirect

Continental Shelf Research

journal homepage: www.elsevier.com/locate/csr

Extreme westward surface drift in the North Sea: Public reports of stranded drifters and Lagrangian tracking

E.V. Stanev[a,b,*], T.H. Badewien[b], H. Freund[b], S. Grayek[a], F. Hahner[b], J. Meyerjürgens[b], M. Ricker[b], R.I. Schöneich-Argent[b], J.-O. Wolff[b], O. Zielinski[b]

[a] Institute of Coastal Research, Helmholtz-Zentrum Geesthacht, Geesthacht, Germany
[b] Institute for Chemistry and Biology of the Marine Environment, University of Oldenburg, Oldenburg, Germany

A B S T R A C T

Observations using two kinds of drifters were carried out in the southern North Sea aiming to study the propagation pathways of marine litter. One drifter, which was driven by the upper layer currents, was equipped with Global Positioning System. Further 1600 wooden drifters, mostly driven by wind and Stokes drift, were released offshore in German waters. The detailed reports of stranded wooden drifters from members of the public, the majority of which are likely to be non-scientists, provided a valuable contribution to the drifter experiment demonstrating the usefulness of citizen science. In 2018, an extreme wind event reversed the circulation of North Sea for more than a month which resulted in a large number of wooden drifters being washed ashore on the British coast. Lagrangian numerical experiments, calibrated using data from the drifter observations, helped explain the anomalous transport and the reversal of the circulation at the sea surface and in deeper layers. The plausibility of similar events during past decades has also been estimated using data from atmospheric analyses. Events as strong as the one observed in 2018 occurred only four times in the last 40 years.

1. Introduction

The North Sea is a shallow shelf sea across most of its area of 750,000 km^2, with a mean depth of ~90 m and a maximum depth of ~700 m in the Norwegian Trench. It is connected to the Atlantic Ocean through the Norwegian Sea at its northern boundary. From there, tides generate a Kelvin wave which first propagates to the south along the British coast. An important part of the tidal forcing for the North Sea originates from the English Channel, an area with a large tidal range, reaching more than 10 m in some places. The incoming tides (from the north and from the southwest through the English Channel) "synchronise" east of the strait, building a local amphydromy. The Kelvin wave propagates further to the east and north along the coastline of the German Bight and exits the North Sea along the Norwegian Trench. The combination between tidal, wind and buoyancy forcing tends to develop a general anti-clockwise circulation (Mathis et al., 2015). The latter is strongly impacted by river runoff.

Research on the wind effects in the North Sea focused mostly on the annual mean circulation or on the circulation patterns resulting from wind blowing from different directions and with varying magnitudes (Maier-Reimer, 1977; Otto et al., 1990; Backhaus, 1989; Sündermann and Pohlmann, 2011). Recently, Jacob and Stanev (2017) showed that the effects of tides and wind are not just additive, and that the non-linear interactions tended to enhance the mean circulation in the North Sea. This study demonstrated that coupling between circulation, driven by the atmospheric variability, and tides could strongly affect the input of mechanical energy in this tidal basin.

The vertical mixing in the North Sea, which is mostly due to tidal currents, opposes the stabilizing effect of density and tends to create a specific vertical shear of currents manifested by the seasonal migration of tidal fronts. In extensive shallow areas, the upper Ekman layer can reach the bottom. Shear velocity can change in the process of the re-arrangement of the circulation caused by variable winds. However, these processes are not well understood. Observations for vertical current profiles (e.g. from ADCP) over wider areas are still scarce. This hinders the understanding of ocean responses to wind for which we need to know spatial patterns, vertical shear and temporal change. Using co-located measurements from different platforms (e.g. from HF radars and ADCP, see Baschek et al., 2017) improved the quality of surface currents forecasting (Stanev et al., 2015). Yet the understanding of the response processes in a very thin surface layer is limited (Laxague et al., 2018). Not much is known about the role of extreme winds and the resulting reshaping of the circulation in the North Sea. Such knowledge is needed for trajectory forecasts and many related activities, e.g. search and rescue operations (Röhrs et al., 2012), propagation of fish eggs, larvae and marine litter (van der Molen et al., 2007; Christensen et al., 2007; Gutow et al., 2018), or for optimizing the use of the marine environment and preserving its environmental status (Emeis et al., 2015).

* Corresponding author. Institute of Coastal Research, Helmholtz-Zentrum Geesthacht, Geesthacht, Germany.
E-mail address: emil.stanev@hzg.de (E.V. Stanev).

https://doi.org/10.1016/j.csr.2019.03.003
Received 8 December 2018; Received in revised form 5 February 2019; Accepted 8 March 2019
Available online 16 March 2019

The present work was motivated by observations made during the project “Macroplastics Pollution in the Southern North Sea” (http://www.macroplastics.de/), one aim of which was to study the propagation pathways of marine litter in the North Sea. One way to do this is to use surface drifters which are advected by the Lagrangian current that includes the wave-induced Stokes drift. Drifter observations (Meyerjürgens et al., 2019; see also http://portal.macroplastics.de/index.php?page=drifter-meldung) revealed, among others, an anomalous westward propagation during February/March 2018. Drifters released within a distance of 40–120 km to the German coastline stranded at the east coast of England and Scotland. This is contrary to the “canonic” circulation scheme described above. A simple explanation for this finding could be that easterlies persisted for a relatively long time after the release of the drifters. However, wind is not the only driving factor. The drift velocities also depend on how drifters respond to surface waves and ocean currents (Daniel et al., 2002; Breivik and Allen, 2008; Röhrs et al., 2012). The contributions of these three factors are different depending on the specific drifter. Negative (positive) buoyancy would tend to keep a drifter near the bottom (surface) therefore the response to flow convergence (divergence) can differ for different drifters. Our specific objectives were to: (1) explain the observed anomalous transport, (2) analyze the reversal of the circulation at the sea surface and in deeper layers, and (3) quantify the plausibility of similar events to have occurred in the past.

The methods applied use a combination of observations, data from operational ocean models and Lagrangian modelling. For a recent review on Lagrangian ocean analysis the reader is referred to van Sebille et al. (2018). The present paper is organized as follows: The observational and numerical methods used are described, followed by the analysis and results. A discussion on anomalous conditions for westward propagation in the past and short conclusions are given at the end.

2. Methods

2.1. Wooden drifters

A total of 1600 wooden drifters were released during the research cruise HE503 of the RV Heincke. The first release of 800 wooden drifters was carried out on 24.02.2018 in the southern North Sea at approximately 53.78° N, 6.42° E (Borkum Riffgrund, red circle in Fig. 1) which is situated northwest of the Dollart, i.e. the Ems estuary. The second release of 800 wooden drifters was conducted on 27.02.2018 at approximately 54.97° N, 6.79° E (Sylter Außenriff, black circle in Fig. 1).

The wooden drifters are cut from solid, FSC-certified spruce wood, and measure 10 × 12 cm. Finders are asked to report the drifters via the project website (Aden and Stephan, 2017). Hence, a message in German and English as well as a unique identification number are branded on either side (Fig. 2a). Each report contains information on the drifter ID, the location and time of finding, as well as any additional comments that the finder may want to leave.

For the purpose of this study, data validation and analyses were carried out on all records up until 05.06.2018. Data validation included the removal of all copies of any particular record if these copies were the result of a finder entering the same information several times in a row. Multiple reports of the same drifter were not deleted if there was a difference in finding date, time or location. Reports that were not recorded on the coastline or within a seaward distance of 500 m were checked for comments indicating the correct finding location. If such information was given, the report point was repositioned accordingly. Some drifters were indeed found at sea by sailors, sea kayakers or in fishing trawls. These reports were retained in the record. If there was no further information available, the record was deleted. The seaward distance of 500 m was chosen as this seemed a reasonable distance for walks across the mudflats at low tide.

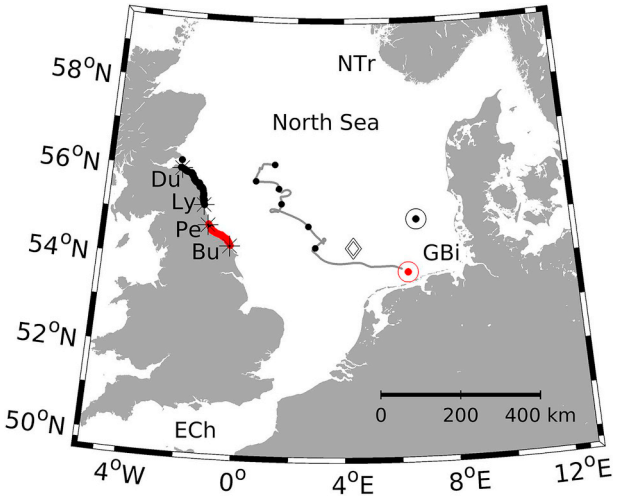

Fig. 1. Overview of the study area and specific locations. Locations where drifters were released in the German Bight are shown with big circular symbols. The ones released on 24.02.2018 at Borkum Riffgrund are shown with red symbols, the ones released on 27.02.2018 at Sylter Außenriff with black symbols. Locations where drifters were found on the British coast are shown with small circle symbols. The trajectory of one GPS drifter is also shown from 24.02 to 25.04.2018. Every 10th day is marked on the trajectory with a small circle symbol. A selected location (54.33° N, 4.33° E) for which data analysis is presented in the text is shown with a diamond-shaped symbol. The following abbreviations are used: *Dunbar* (Du), *Lynemouth* (Ly), *Peterlee* (Pe) and *Burniston* (Bu), *English Channel* (ECh), *German Bight* (GBi) and *Norwegian Trench* (NTr). (For interpretation of the references to color in this figure legend, the reader is referred to the Web version of this article.)

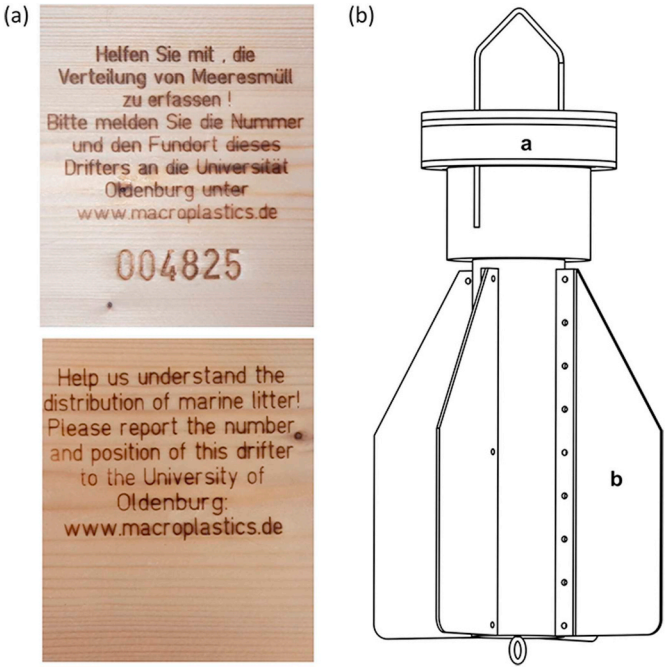

Fig. 2. (a) Top view of the front and back of the drifters which are branded with a unique identification number as well as the request to each finder in German and English. (b) GPS drifter.

2.2. GPS drifters

GPS drifters were constructed at the University of Oldenburg to be used as part of the research project (Meyerjürgens et al., 2019). The cylindrical shaped housing (500 mm in length) of the drifters is made of polyvinyl chloride (PVC) and is divided into two parts (Fig. 2b). The

upper part (140 mm in diameter, marked with "a" in the figure) holds the positioning and transmission unit and is surrounded by a Styrofoam ring for a positive buoyancy to keep the drifter in an upright position in the water. The lower part (90 mm in diameter) contains a battery pack which powers the GPS transmitter, yielding an average battery life span of 4 months by transmitting the positions at an interval of 10 min. The drifters are designed to follow the current of the upper 0.5 m of the surface layer. Four drag-producing cruciform wings (marked with "b" in the figure) are mounted directly to the lower part of the housing to reduce the direct windslip-induced motion to the drifter.

In this study, we use the positions of one drifter that was deployed at the same time and location (for coordinates, see section 2.1) as the wooden drifters at Borkum Riffgrund. Positions of the drifter were sampled with an accuracy of ~2.5 m. Outliers in the drifter time-series data were eliminated with a Hampel median filter (Liu et al., 2004) using a window size of nine and a tolerance of three standard deviations. Since drifter positions were measured at irregular time intervals, the position data were interpolated using a piecewise cubic interpolation method, creating a consistent data output at 10-min intervals. The interpolated positions were then low-pass filtered (with a cut-off period at two M2 periods) to remove high frequency components, such as tidal currents and inertial motions, from the position time series data.

2.3. Numerical modelling

2.3.1. Data from operational models

Start and end positions and times are the only information known for the wooden drifters. The GPS drifter also provides the trajectory, but does not fully describe the circulation in the North Sea. Therefore, for the period of drifter observations, data from the CMEMS numerical model for the European North West Shelf (NWS) were also used. From all available data, we considered atmospheric pressure (needed to describe the atmospheric conditions), 10 m wind and currents. The numerical model is known as NWS FOAM-AMM7, which is based on version 3.6 of NEMO (Madec, 2008). The last index "7" indicates that the horizontal resolution is ~7 km (1/9° in longitude and 1/15° in latitude). The model has 51 hybrid s-σ-layers (Siddorn and Furner, 2013). It is one-way nested to a global ocean model. A 3DVar system is used for the assimilation of sea surface temperature data. Model validation is documented by O'Dea et al. (2012). For the present Lagrangian simulations, we used hourly data from a section of the model domain (−5.50 to 13.00°E, and 49.50 to 59.50°N).

The second set of data from operational modelling included Stokes drift velocities. These are produced from the North-West European Shelf Wave Analysis and Forecast system using the WAVEWATCH III model (version 4.18, The WAVEWATCH III Development Group, 2016). The model is set up for the area of AMM7, uses the same bathymetry as the AMM7 model and is known as the WWIII-AMM7 model. The effect of currents from the NWS FOAM-AMM7 model on the waves are included. The wave model is nested into a global wave model; the latter provides boundary conditions as wave spectra.

2.3.2. Lagrangian modelling

Particle tracking was used to analyze the transport in the studied area and to support the observations from the GPS and wooden drifters. Experiments were carried out "offline" using data from the circulation and wave model, as well as 10 m winds. The formulation of the velocity, which drives the floating objects, will be given later. The model is the freely available open-source model OpenDrift (Dagestad et al., 2017), which uses a 2nd-order Runge-Kutta scheme. The coefficient of horizontal diffusion is considered as a function of grid size Δl:

$$A_H = c_1 * \Delta l^{\frac{4}{3}} \quad (1)$$

From diffusion experiments (Okubo, 1971; Weidemann, 1984), c_1 was specified as $1.1 \times 10^{-4}\,m^{2/3}\,s^{-1}$. Velocities representing the turbulent particle advection by random walk displacements were computed as:

$$u'(t) = \sqrt{\frac{2A_H}{dt}}\,R_x(t) \quad (2)$$

$$v'(t) = \sqrt{\frac{2A_H}{dt}}\,R_y(t) \quad (3)$$

where R_x and R_y are independent random numbers from a normal distribution with zero mean and variance one. Further details can be found in Schönfeld (1995) and Callies et al. (2011), both using this approach of parameterizing horizontal diffusion for particle advection. The time-step is dt = 10 min and the output is also written every 10 min.

2.3.3. Experiments

The Lagrangian experiments described below help to address the first and second objective formulated in the introduction, namely to adequately simulate the observed anomalous transport and the reversal of the surface circulation in early 2018. These experiments relate to the observations from the deployed surface drifters (for the specific period during which these observations were made). Reversals of the circulation in deeper layers and long-term changes that precede the time frame between February and June 2018 are based on Eulerian analyses.

The particle tracking experiments aim to: (1) calibrate the simulations in order to optimize the replication of the observed GPS drifter movement; (2) analyze the trajectories of Lagrangian particles with the same characteristics as the GPS drifter over the entire model area; (3) use particle tracking to simulate the trajectories of the wooden drifters. Therefore three seeding experiments were performed:

1. Simulation of the GPS drifter,
2. Domain-wide, uniform initial distribution seeding with 1 particle per model grid, and
3. Simulation of the wooden drifters following the two releases described in Sect. 2.1.

The results of experiment-1 were used to calibrate the wind drag in experiment-2. In experiment-2 12,107 particles were advected for 30 days. No stranding was allowed for these particles. In experiment-3, particles resembling the wooden drifters were allowed to strand. Their initial distribution followed a normal distribution law. Sixty-eight percent of the particles were located within a radius of 500 m from the location of the real release. Their tracking continued until 30.04.2018. This time was consistent with the maximum finding time reported for the British coast. In the simulations, all particles stranded before this date.

3. Results

3.1. Analysis of meteorological and oceanographic conditions

Data analyzed below is extracted from the ERA5 data set. The weather situation after the first release of drifters was dominated by a high pressure system over Scandinavia with a passing low pressure system in the northern Atlantic Ocean, 20° west of the United Kingdom. Another depression passed by west of the Iberian Peninsula during the second release of drifters and was accompanied by the high pressure system over Scandinavia. This pattern resulted in persistent easterly winds in the whole North Sea basin (Fig. 3a) during and after the drifter releases. These events are known as the 'Beast from the East', a phrase used to describe cold conditions in the UK caused by easterly winds from the continent. A day before the second release of wooden drifters, the temperature was −7.5 °C and it was always below 0 °C during research cruise HE503.

The directions in which the wind blew between 24.02. and

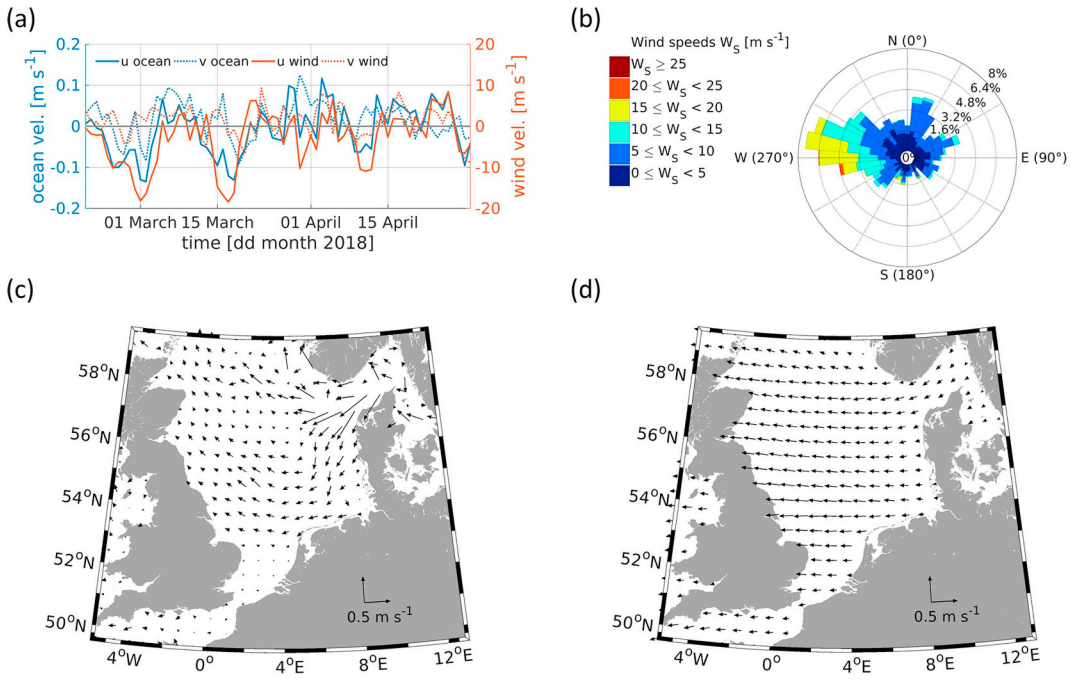

Fig. 3. Temporal evolution of daily mean x and y components of wind and surface currents (see legend) in the location shown in Fig. 1 with a diamond-shaped symbol during the time period 19.02.-30.04.2018 (a). Wind rose showing directions in which the wind blew during the same period (b). Daily mean surface current and Stokes drift, are shown in (c) and (d), respectively, in every 7th model grid in each direction during the time of maximum easterly wind (19.02.2018–08.03.2018).

25.06.2018 as well as the respective wind speed distribution are shown in Fig. 3b for a location in the middle of the southern North Sea (see the diamond-shaped symbol in Fig. 1). This location was chosen to be representative for the region in which the drifters propagated, as well as for the overall hydrological and meteorological conditions in the area of this study. The general wind direction was mostly towards west with peak values of up to 22.6 m s^{-1}. The time period 19.02.-30.04.2018 exhibited the strongest easterlies. Ocean surface velocities responded to the wind speeds which resulted in a general westward ocean surface circulation accompanied by westward Stokes Drift velocities. This is also illustrated by the mean velocities of surface currents and Stokes Drift in Fig. 3 c, d.

3.2. Drifter observations

In total, 782 validated drifter reports were recorded until 05.06.2018 (Table 1). All of these reports were made along the British northeast coast (Fig. 1). Out of these, 426 drifters were registered from the first batch, released at Borkum Riffgrund. The first report of ten drifters from this group occurred on 09.03.2018, i.e. 13 days after the release. The finding spot near Redcar in North Yorkshire (see Fig. A1, where all geographic names mentioned in the text are shown) is located 501.50 km from the release position. The respective mean drifter velocity was therefore ~0.5 m s^{-1}. The majority of findings, i.e. 288 reports (67.61%) were made during the second week after the first discovery, i.e. 16.-23.03.2018 (Table 1). Of all registered drifters from the first batch, 331 drifters were reported once, 40 reported twice, one drifter was logged at three different times and positions, and three drifters were reported four times each. This equates to 375 unique drifter IDs and a retrieval rate of 46.88%. The shortest geodesic distance that these drifters floated was 451.51 km, the longest 559.45 km. The total linear coastline of 162.61 km over which drifters released at Borkum Riffgrund were discovered, stretches between Seahouses and Burniston, north of Scarborough. Excluding the northernmost report near Seahouses, 374 of the drifters were discovered over a geodesic distance of 76.84 km between Peterlee and Burniston (Fig. 1 and Fig. A1).

Table 1
The number of reported drifters (n) from either of the two releases over a period of 13 weeks following the first discovery.

Week	release 1		release 2	
	Dates	n reports	Dates	n reports
1	09.03.-16.03.	13	18.03.-25.03.	1
2	17.03.-23.03.	288	26.03.-01.04.	3
3	24.03.-30.03.	57	01.04.-08.04.	148
4	31.03.-06.04.	31	09.04.-15.04.	126
5	07.04.-13.04.	16	16.04.-22.04.	25
6	14.04.-20.04.	1	23.04.-29.04.	17
7	21.04.-27.04.	2	30.04.-06.05.	13
8	28.04.-04.05.	1	07.05.-13.05.	6
9	05.05.-11.05.	8	14.05.-20.05.	2
10	12.05.-18.05.	7	21.05.-27.05.	6
11	19.05.-25.05.	0	28.05.-03.06.	9
12	26.05.-01.06.	2	04.06.-05.06.	0
13	02.06.-05.06.	0	N/A	N/A
total		426		356

From the 800 drifters released at the Sylter Außenriff, a total of 356 reports were recorded. The first one was found after 19 days on 18.03.2018 in Hartlepool, which is also the closest from its release position, 514.54 km away. Most reports were registered via the website in the third (n = 148) and fourth week (n = 126; 76.97%) after the initial finding, i.e. between 01. and 15.04.2018 (Table 1). 248 drifters were reported once, 43 reported twice, six three times and one drifter was found and reported at four instances. With 298 unique drifter IDs, the retrieval rate for this offshore release therefore results in 37.25%. The furthest geodesic distance covered by any drifter from this second offshore batch was 604.15 km. The total linear coastline stretch over which drifters released at the Sylter Außenriff were discovered, measures 186.35 km between the Isle of May and Hartlepool. Excluding the southernmost drifter report in Hartlepool Marina, 297 of the drifters were found over a linear, geodesic distance of 125.80 km between

Dunbar and Lynemouth (star symbols in Fig. 1).

The trajectory of the GPS drifter (grey solid line in Fig. 1) complements the propagation patterns of floating objects. The strong easterly wind conditions resulted in an overall westward displacement. Ten days after its release, it drifted slowly to the north-east. During the two months considered here, it covered a distance of 425 km.

3.3. Lagrangian simulations

3.3.1. Rationale

The motion of drifters depends on the Eulerian surface current, Stokes drift and direct wind effects, for which some examples exist, e.g. Ardhuin et al. (2009) who estimated surface current and waves motion using HF radar data. Simpler approaches account for the wave effects using parameterizations based on wind only without using a separate wave model. However, such parameterizations assume a local correlation between wind and waves, which is often not the case, as stressed by Röhrs et al. (2012) who analyzed in situ measurements of currents, waves and drifter trajectories. Their conclusion was that a young wind-sea is characterized by short waves with high Stokes drift speeds and large vertical shear. Swell conditions are characterized by a Stokes drift profile that is more uniformly distributed with depth. In line with the conclusion of Röhrs et al. (2012) that "the predictability of drift trajectories can be improved by adding wave information from a numerical wave model", we used the data described in Section 2.3.1, whereby the effect of currents on the waves were included.

The more challenging part of the problem is that the motion of drifters not only depends on the Eulerian current, Stokes drift and direct wind drag. The combination between these three forcing factors is also influenced by the type of drifter. As demonstrated by Röhrs et al. (2012), different drifter types respond differently to wind events. This response is not uniform for distinct conditions. As these authors showed, the onset of strong wind could change the responses. Different shear velocities during varying wind situations give one explanation of this effect. As shown in section 3.2, the GPS drifter is less exposed to direct wind effects in comparison to the wooden drifters which are not fully submerged.

3.3.2. GPS drifter

Our observations do not provide enough independent data, e.g. for shear velocity, for a precise calibration. Therefore we carried out a number of Lagrangian experiments by adding different percentages of wind velocity to the sum of surface current and Stokes drift velocity. The comparison between observed and simulated trajectories in experiment-1 demonstrated that during strong wind events, the Stokes drift has comparable magnitudes, or even exceeds the Eulerian mean current (Fig. 3c and d). This is consistent with the observations of Röhrs et al. (2012).

Velocities estimated from the simulated and real drifters were compared for different coefficients of wind drag, and the coefficient corresponding to the minimum root mean square (rms) difference was chosen as the most appropriate one. The corresponding "optimal" results are shown in Fig. 4a and Fig. 4d for the zonal and meridional velocity component. The skill of simulations was estimated by the index of agreement $= 1 - \frac{\sum_{i=1}^{n}(P_i - O_i)^2}{\sum_{i=1}^{n}(|P_i - \bar{O}| + |O_i - \bar{O}|)^2}$, where, n is the number of observations (index i) and the overbar is the temporal mean of the observed data (Willmott, 1981). This index quantifies the degree to which the observed data O is estimated by the predicted value P (1 indicates a perfect agreement, 0 indicates no agreement at all). The resulting index of agreement of $D = 0.98$ and the correlation between observations and simulations of 0.97 are quite good given that the error is relatively small compared to the squared variance of velocity. This agreement adequately demonstrates the high data quality from the operational models.

The comparison between the skills for the zonal (meridional) velocity in Fig. 4a(b) and Fig. 4d(e) resulting from the experiments with different wind drag coefficients (0.3% and 1%) demonstrates that an increase of the wind drag coefficient to 1% does not improve the statistics (the index of agreement drops to $D = 0.95$). The conclusion is that the GPS drifter can be considered to be primarily driven by the Eulerian currents and Stokes drift because the direct wind drag (0.3%) is negligible. Wind waves however appear to be important contributors, as seen in Fig. 4c and f, where the Stokes drift has been omitted. Statistics are not shown for these latter figures because they are uninformative if an important transport mechanism has been omitted in one of the data sets.

The contributions from the Eulerian near-surface current, direct wind drag, and Stokes drift are quantified below in an Eulerian framework for the location shown with the diamond-shaped symbol in Fig. 1. Here the velocity is integrated in time to yield the individual contributions of three driving terms to the zonal displacement in a time frame comparable to the observation periods. In the case of the best skill (the coefficient of wind drag is 0.3%) the contribution of the direct wind drag (green line in Fig. 5) is essentially smaller than the one of the surface current (black line in Fig. 5) and that of the Stokes drift (red line in Fig. 5). If the Stokes drift was unknown, wind drag would have to be increased to ~1.3% of wind velocity. In this case (blue line in Fig. 5), the integrated velocity would almost coincide with the one computed using Eulerian surface current, Stokes drift, and direct wind drag.

The reason why all curves in Fig. 5 start from negative values is that the integration is performed for a longer period of time. The non-parallel course of the curves corresponding to the wind drag and Stokes drift (Fig. 5) is instructive that the effect of waves could change during different wind conditions.

The velocity at a single point gives only local estimates because the Eulerian near-surface current, direct wind drift, and Stokes drift vary spatially. In order to show the "real-world analogue" of Fig. 4, we changed the framework from Eulerian to Lagrangian. With the optimal wind drag of 0.3%, Fig. 6 shows the simulated propagation of model drifters with the characteristics of the GPS buoy, which originate in any given grid cell, accounting for spatial changes in the local current, wave, and wind fields as the particle moves on its way over the entire North Sea (experiment-2). Many of the particles covered distances of more than 400 km, which is ~2/3 of the zonal size of the North Sea.

3.3.3. Wooden drifters

The calibration of wind drag for the wooden drifters (experiment-3) was conducted by comparing the simulated stranding positions with the real ones and finding the appropriate coefficient for which the difference between stranding positions of real and simulated drifters were minimum.

For these drifters which are much more exposed to the wind, the additional contribution of the wind to the current and Stokes drift is estimated at ~2.5%. The movement of simulated drifters (Fig. 7) gives an idea of the irregular drift (in time) due to the two strong wind pulses (Fig. 3a). The first pulse lasted for approx. 10 days and resulted in a continuous displacement of those drifters released at Borkum Riffgrund up to the western coasts of the North Sea (see the southern pathway in Fig. 7). Shortly after 06.03., the wind subsided and it took another ~10 days for these drifters to strand between Burniston and Peterlee.

The release at the Sylter Außenriff site occurred three days later than the first one, and by 04.03., the respective drifters (black in Fig. 7) covered less than half the distance between the eastern and western North Sea coasts. At that time, the wind decreased (Fig. 3a) and the drifters stagnated in the centre of the basin for about 10 days. The second wind pulse transported them close to the UK's eastern coast in approx. 5 days. However, wind conditions became very variable, velocities decreased (see Fig. 3a) and it took ~20–25 further days after 19.03. for the wooden drifters to strand (note the back and forth movement of the cloud of drifters in the proximity of the coast).

The stranding positions of model drifters with characteristics of the

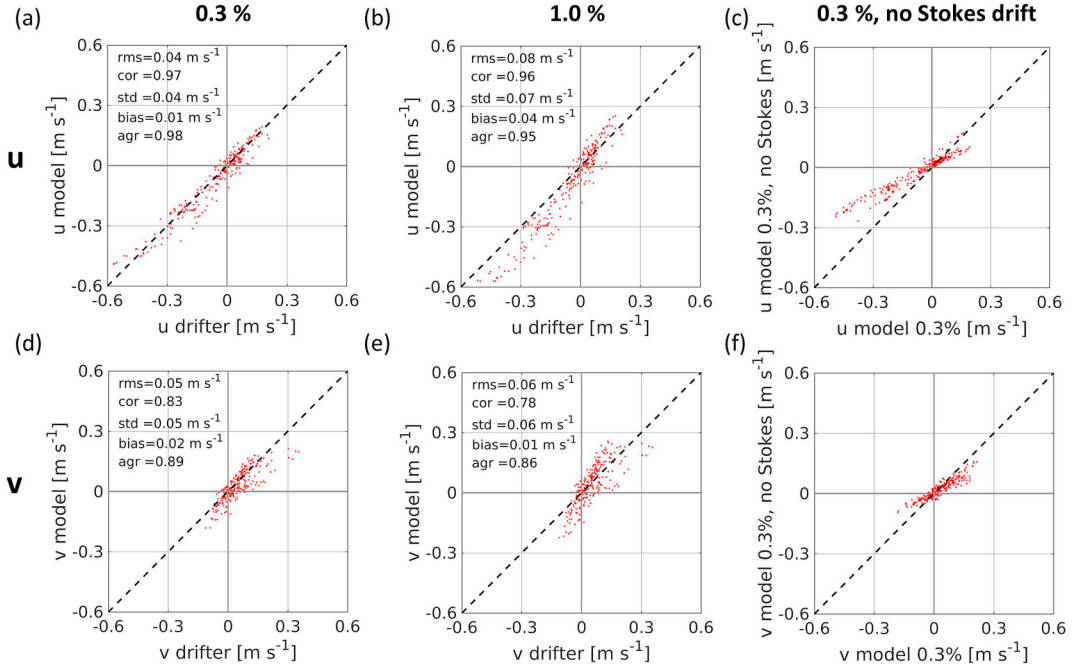

Fig. 4. Simulated (y-axis) versus observed (x-axis) velocities of GPS drifter. Top: u-component, bottom v-component. In the panels on the left the coefficient of wind drag is 0.3%, in the panels in the middle this coefficient is increased to 1%, in the panels on the right Stokes drift is not included. The analysis is based on detided observations and model data. The abbreviations in the legends are as follows: rms - root mean square difference, cor – correlation, std – standard deviation, agr – coefficient of agreement.

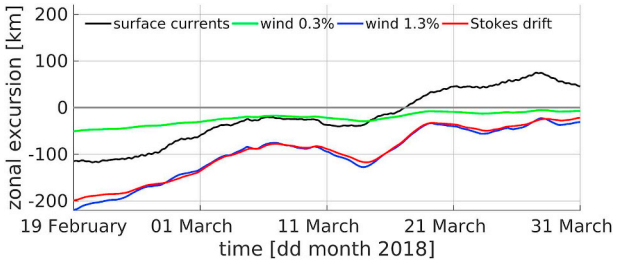

Fig. 5. Zonal velocity integrated in time from 19.02 to 31.03.2018 (zonal excursion) in the location denoted by the diamond-shaped symbol in Fig. 1. The individual curves correspond to excursions caused by ocean surface currents (black line), 0.3% wind (green), 1.3% wind (blue) and Stokes drift (red). (For interpretation of the references to color in this figure legend, the reader is referred to the Web version of this article.)

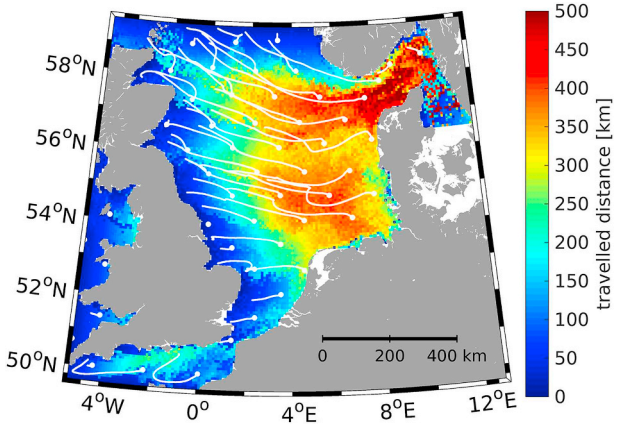

Fig. 6. Displacement of particles from their seeding position over 30 days of integration of the Lagrangian model (19.02.-21.03.2018). The color scale represents the respective distance (lengths of great circle arcs) between the release location and the final position. Exemplary trajectories (64 out of 11,969 in total) are also shown in white. White circles indicate the initial positions. These particles have the properties of the GPS drifter. (For interpretation of the references to color in this figure legend, the reader is referred to the Web version of this article.)

wooden drifters from the two releases (Fig. 7) coincided almost perfectly with the observations (Fig. 1). Furthermore, simulated stranding times matched the data in Table 1. Although the reporting time of the wooden drifters can be quite different from their stranding time, there is a reasonable correspondence with model estimates. Almost all wooden drifters released at the Sylter Außenriff stranded in week 3 (n = 148) and 4 (n = 126). The majority of simulated drifters also stranded in week 3 (n = 404) and 4 (n = 395).

3.4. Pronounced reversals of the North Sea circulation

The observed westward transport in the southern North Sea after the drifters had been released can be mostly attributed to wind and Stokes drift. This is well illustrated in Fig. 5, in which the zonal velocity component (integrated in time over one month) due to Eulerian surface current, Stokes drift and wind (at 0.3%) are shown for the selected position (diamond-shaped symbol in Fig. 1). After one month of integration, the current yielded a westward displacement of ~110 km, Stokes drift of ~200 km and wind drag of ~50 km, altogether a distance of ~360 km.

From the above analysis, it is not clear whether these extreme events resulted in a substantial re-arrangement of the circulation in the North Sea throughout the water column. Neither the drifter observations nor the model data covering the entire North Sea are available over extended periods of time, which makes the diagnostics of past changes, in particular in a Lagrangian framework, particularly challenging. In order to address past changes of the circulation, we used the Eulerian framework once more for the location denoted by the diamond-shaped symbol in Fig. 1. The respective mean surface current in this location compares well with the generally accepted value of a mean eastward surface current of ~3 cm s^{-1} (Sündermann and Pohlmann, 2011). However, the events in early 2018 can be considered extreme,

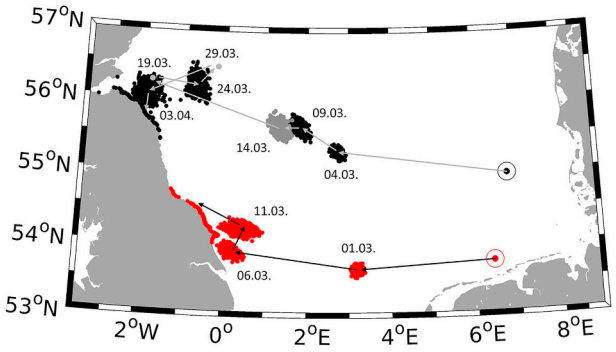

Fig. 7. Positions of the model wooden drifters every 5th day after their release at the Borkum Riffgrund site (big red circle) and the Sylter Außenriff site (big black circle). The simulated particles are shown with the color of the respective release position. Because of the partial overlap of positions on 09. and 14.03., grey and black are used. From 19.03.-03.04., drifters from the Sylter Außenriff stagnated in a relatively small area, therefore only the approximate positions of the centre of the particle clouds have been shown for 19.03. and 29.03. The stranding positions of model wooden drifters are also shown (red and black dots on the coast). (For interpretation of the references to color in this figure legend, the reader is referred to the Web version of this article.)

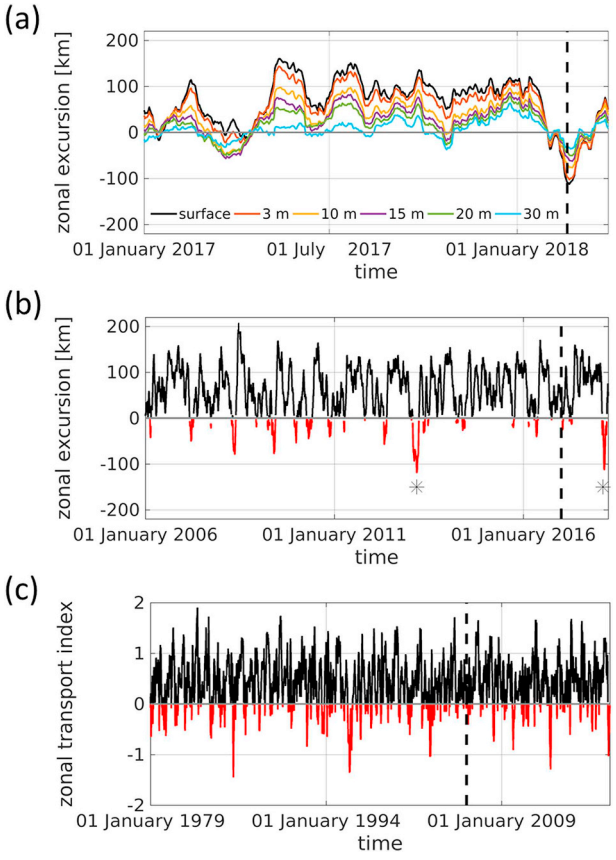

Fig. 8. (a) Zonal velocity integrated during the period 01.01.2017–31.03.2018 (zonal excursion), caused by ocean currents at different depths. (b) Zonal excursion caused by surface currents for the period 01.01.2006–31.03.2018. Negative values are in red. Star-symbols identify the two major reversals of circulation. (c) Zonal transport index, as defined at the end of section 3.4, from 01.01.1979 to 31.03.2018. Vertical dashed lines identify the zooming into and out of the time-axis: the period shown in Fig. 5 is a high-resolution view of the area to the right of the dashed line shown in (a); the period shown in (a) represents the section of the graph to the right of the dashed line shown in (b); the period shown in (b) is the high-resolution subset of the graph to the right of the dashed line shown in (c). (For interpretation of the references to color in this figure legend, the reader is referred to the Web version of this article.)

resulting in a pronounced below-surface response to easterly winds (notice the individual curves in Fig. 8a). Therefore it can be concluded, that the discussed extreme event reversed the circulation in the North Sea down to the seabed.

One reasonable question is whether such extreme weather conditions could result in frequent reversals of the zonal transport in the North Sea. Nowadays, data from operational models are available for relatively long periods of time (http://marine.copernicus.eu/), thus the analysis shown in Fig. 8a can be presented for decadal periods (Fig. 8b). Considering the current decade, a reversal of the surface circulation of the magnitude recorded for early 2018 occurred only twice.

Similar estimates can be made for longer periods based on available wind data only, knowing that the water excursion due to surface current is about 0.4 times that caused by wind drag and Stokes drift. One can thus use wind data from long-term atmospheric reanalyses to estimate the surface drift. In order to relate past events to the one observed in 2018, we defined a zonal transport index as the ratio between the westward excursion of ~200 km caused by Stokes drift in 2018 and the zonal excursion at any time computed from wind data only. This index allows to identify similar extreme events in the past (Fig. 8c). In the last forty years there were only four events stronger than the one observed in 2018.

4. Discussion

Tides are responsible for the back and forth motion of the North Sea water masses. The tidal excursions range from zero (in amphidromic points) to ~20–30 km in the coastal areas. This is an order of magnitude larger than the transport by mean currents. Analyses shown above demonstrated that synoptic winds could result in much longer excursions of water particles at the ocean surface of ~50–100 km per week. Keeping in mind that wind is usually not uniform and that it changes over time, one may expect that a wind-induced circulation could substantially change the geometric extension and shape of dominant water masses. This calls for a more profound model-based investigation of oceanic responses to synoptic forcing from the atmosphere and associated longer-term anomalies in the atmospheric forcing.

The consequences of the reshaping of the North Sea circulation pattern caused by synoptic and extreme winds is important not only when addressing search and rescue operations or propagation of marine litter. It could play an important role in the process of the re-arrangement and evolution of fronts and biogeochemical properties of this shallow basin. Although wind-driven circulations seem to have been widely studied in the past, further research from a Lagrangian perspective could be particularly interesting when coupled with other (e.g. biogeochemical) processes.

The key finding of this present study, i.e. the persistent reversal of the North Sea circulation (for about 1.5 months), triggered by strong winds with a pronounced westward component and with approximately the same duration, appears to be a significant event in this basin. No less impressive is the fact that non-scientists substantially helped to identify it. Although extreme westward drift of the magnitude observed here rarely takes place (four times in the last forty years), it is important to understand the possible consequences, including expected changes in the ocean state from the point of view of physics and biogeochemistry. The recovery of the North Sea system back to its normal state after such extreme events also deserves a profound investigation.

5. Conclusions

Drifter releases were conducted in early 2018 in German waters using one drifter equipped with Global Positioning System, as well as 1600 wooden drifters. Some of these stranded in different coastal areas. This unique exercise appeared successful because individuals finding the stranded objects gave their valuable feedback about position and time of drifter findings. This public participation in scientific research

demonstrated the usefulness of citizen science.

An anomalous propagation of the drifters was observed. Some of them reached the British coast in just a few weeks. Using observed and numerically simulated drifters allowed us to calibrate the Lagrangian model in a way to adequately resolve the wind drag. This further enabled us to reconstruct the propagation pathways during the period of strong easterlies in early 2018.

The analyses of long-term current and wind data demonstrated that intermittent extreme events such as the one in 2018 resulted in a substantial reshaping (reversal) of the North Sea circulation.

Acknowledgements

The authors are grateful to all people finding and reporting drifters. We thank Nathan Laxague and one anonymous reviewer for the useful comments. Data from CMEMS portal for the European North West Shelf (NWS) have been used. This work was carried out within the project "Macroplastics Pollution in the Southern North Sea - Sources, Pathways and Abatement Strategies" (grant no. ZN3176), funded by the Ministry of Science and Culture of the German Federal State of Lower Saxony. SG acknowledges funding from the European Union's Programme for Research, Technological Development and Demonstration under grant agreement no. H2020-EO-2016-730030-CEASELESS.

Appendix 1

Fig. A1. Map with geographic names referred to in this article.

References

Aden, C., Stephan, K., 2017. Web-based citizen involvement in research into pathways and hotspots of marine litter in the southern North sea. In: In: Car, A., Strobl, J., Jekel, T., Griesebner, G. (Eds.), (Hrsg.): GI_Forum - Journal for Geographic Information Science, vol. 2. pp. 60–77.

Ardhuin, F., Marie, L., Rascle, N., Forget, P., Roland, A., 2009. Observation and estimation of Lagrangian, Stokes, and Eulerian currents induced by wind and waves at the sea surface. J. Phys. Oceanogr. 39 (11), 2820–2838. https://doi.org/10.1175/2009JPO4169.1.

Backhaus, J., 1989. The North sea and the climate. Dana A J. Fish. Mar. Res. 8, 69–82.

Baschek, B., Schroeder, F., Brix, H., Riethmüller, R., Badewien, T.H., Breitbach, G., Brügge, B., Colijn, F., Doerffer, R., Eschenbach, C., Friedrich, J., Fischer, P., Garthe, S., Horstmann, J., Krasemann, H., Metfies, K., Merckelbach, L., Ohle, N., Petersen, W., Pröfrock, D., Röttgers, R., Schlüter, M., Schulz, J., Schulz-Stellenfleth, J., Stanev, E., Staneva, J., Winter, C., Wirtz, K., Wollschläger, J., Zielinski, O., Ziemer, F., 2017. The coastal observing system for northern and arctic seas (COSYNA). Ocean Sci. 13, 379–410. https://doi.org/10.5194/os-13-379-2107.

Breivik, O., Allen, A.A., 2008. An operational search and rescue model for the Norwegian Sea and the North Sea. J. Mar. Syst. 69 (1–2), 99–113. https://doi.org/10.1016/j.jmarsys.2007.02.010.

Callies, U., Plüß, A., Kappenberg, J., Kapitza, H., 2011. Particle tracking in the vicinity of Helgoland, North Sea: a model comparison. Ocean Dynam. 61 (12), 2121–2139. https://doi.org/10.1007/s10236-011-0474-8.

Christensen, A., Daewel, U., Jensen, H., Mosegaard, H., St. John, M., Schrum, C., 2007. Hydrodynamic backtracking of fish larvae by individual-based modelling. Mar. Ecol. Prog. Ser. 347, 221–232.

Dagestad, K.-F., Röhrs, J., Breivik, Ø., Ådlandsvik, B., 2017. OpenDrift v1.0: a generic framework for trajectory modeling. Geosci. Model Dev. Discuss. (GMDD) 2017, 1–28. https://doi.org/10.5194/gmd-2017-205.

Daniel, P., Jan, G., Cabioc'h, F., Landau, Y., Loiseau, E., 2002. Drift modeling of cargo containers. Spill Sci. Technol. Bull. 7 (5–6), 279–288. https://doi.org/10.1016/S1353-2561(02)00075-0.

Emeis, K., van Beusekom, J., Callies, U., Ebinghaus, R., Kannen, A., Kraus, G., et al., 2015. The North sea — a shelf sea in the anthropocene. J. Mar. Syst. 141, 18–33. https://doi.org/10.1016/j.jmarsys.2014.03.012.

Gutow, L., Ricker, M., Holstein, J.M., Dannheim, J., Stanev, E.V., Wolff, J.-O., 2018. Distribution and trajectories of floating and benthic marine macrolitter in the south-eastern North Sea. Mar. Pollut. Bull. 131– A, 763–772.

Jacob, B., Stanev, E.V., 2017. Interactions between wind and tidally induced currents in coastal and shelf basins. Ocean Dynam. 67, 1263–1281. https://doi.org/10.1007/s10236-017-1093-9. 2017.

Laxague, N.J.M., Özgökmen, T.M., Haus, B.K., Novelli, G., Shcherbina, A., Sutherland, P., Guigand, C.M., Lund, B., Mehta, S., Alday, M., Molemaker, J., 2018. Observations of near-surface current shear help describe oceanic oil and plastic transport. Geophys. Res. Lett. 45, 245–249. https://doi.org/10.1002/2017GL075891.

Liu, H., Shah, S., Jiang, W., 2004. Online outlier detection and data cleaning. Comput. Chem. Eng. 28, 1635–1647.

Madec, G., 2008. NEMO ocean engine. Note du Pôle de modélisation. Institut Pierre-Simon Laplace (IPSL), France (27).

Maier Reimer, E., 1977. Residual circulation in the North Sea due to the M2-tide and mean annual wind stress. Deutsche Hydrografische Zeitschrift 30 (3), 69–80. https://doi.org/10.1007/BF02227045.

Mathis, M., Elizalde, A., Mikolajewicz, U., Pohlmann, T., 2015. Variability patterns of the general circulation and sea water temperature in the North Sea. Prog. Oceanogr. 135, 91–112. https://doi.org/10.1016/j.pocean.2015.04.009.

Meyerjürgens, J., Badewien, T.H., Garaba, S.P., Wolff, J.-O., Zielinski, O., 2019. A state-of-the-art compact surface drifter reveals pathways of floating marine litter in the German Bight. Front. Mar. Sci. 6, 58. https://doi.org/10.3389/fmars.2019.00058.

Okubo, A., 1971. Oceanic diffusion diagrams. Deep Sea Res. Oceanogr. Abstr. 18 (8), 789–802. https://doi.org/10.1016/0011-7471(71)90046-5.

Otto, L., Zimmerman, J., Furnes, G., Mork, M., Saetre, R., Becker, G., 1990. Review of the physical oceanography of the north sea. Neth. J. Sea Res. 26 (2), 161–238. https://doi.org/10.1016/0077-7579(90)90 091-T http://www.sciencedirect.com/science/article/pii/007775799090091T.

O'Dea, E.J., Arnold, A.K., Edwards, K.P., Furner, R., Hyder, P., Martin, M.J., et al., 2012. An operational ocean forecast system incorporating NEMO and SST data assimilation for the tidally driven European North-West shelf. J. Oper. Oceanogr. 5 (1), 3–17. https://doi.org/10.1080/1755876X.2012.11020128.

Röhrs, J., Christensen, K.H., Hole, L.R., Broström, G., Drivdal, M., Sundby, S., 2012. Observation-based evaluation of surface wave effects on currents and trajectory forecasts. Ocean Dynam. 62, 1519–1533. https://doi.org/10.1007/s10236-012-0576-y.

Schönfeld, W., 1995. Numerical simulation of the dispersion of artificial radionuclides in the English Channel and the North Sea. J. Mar. Syst. 6 (5), 529–544. https://doi.org/10.1016/0924-7963(95)00022-H.

Siddorn, J., Furner, R., 2013. An analytical stretching function that combines the best attributes of geopotential and terrain-following vertical coordinates. Ocean Model. 66, 1–13.

Stanev, E.V., Ziemer, F., Schulz Stellenfleth, J., Seemann, J., Staneva, J., Gurgel, K.W., 2015. Blending surface currents from HF radar observations and numerical modelling: tidal hindcasts and forecasts. J. Atmos. Ocean. Technol. 32, 256–281.

Sündermann, J., Pohlmann, T., 2011. A brief analysis of North Sea physics. Oceanologia 53 (3), 2011.

The WAVEWATCH III Development Group, 2016. User Manual and System Documentation of WAVEWATCH III Version 5.16, vol. 329. NOAA/NWS/NCEP/MMAB Technical Note, pp. 326 (+ Appendices).

van der Molen, J., Rogers, S.I., Ellis, J.R., Fox, C.J., McCloghrie, P., 2007. Dispersal patterns of the eggs and larvae of spring-spawning fish in the Irish Sea, UK. J. Sea Res. 58 (4), 313–330.

van Sebille, E., Griffies, S.M., Abernathey, R., Adams, T.P., Berloff, P., Biastoch, A., Blanke, B., Chassignet, E.P., Cheng, Y., Cotter, C.J., Deleersnijder, E., Döös, K., Drake, H.F., Drijfhout, S., Gary, S.F., Heemink, A.W., Kjellsson, J., Koszalka, I.M., Lange, M., Lique, C., MacGilchrist, G.A., Marsh, R., CG Mayorga Adame, R McAdam, Nencioli, F., Paris, C.B., Piggott, M.D., Polton, J.A., Rühs, S., Shah, S.H.A.M., Thomas, M.D., Wang, J., Wolfram, P.J., Zanna, L., Zika, J.D., 2018. Lagrangian ocean analysis: fundamentals and practices. Ocean Model. 121, 49–75.

Weidemann, H., 1984. Tracer diffusion experiments during FLEX '76. Rapp. P.-V. Reun. Cons. Int. Explor. Mer. 185, 39–66.

Willmott, C.J., 1981. On the validation of models. Phys. Geogr. 2 (2), 184–194.